

$\text{Bi}_{2+x}\text{Sr}_{2-x}\text{CuO}_y$ ($0.10 \leq x \leq 0.40$) studied by photoemission and inverse-photoemission spectroscopy

N. Sanada, M. Shimomura, Y. Suzuki, and Y. Fukuda*

Research Institute of Electronics, Shizuoka University, Hamamatsu 432, Japan

M. Nagoshi

Applied Technology Research Center, NKK Corporation, Kawasaki 210, Japan

M. Ogita

College of Engineering, Shizuoka University, Hamamatsu 432, Japan

Y. Syono and M. Tachiki

Institute for Materials Research, Tohoku University, Sendai 980, Japan

(Received 27 August 1993; revised manuscript received 8 November 1993)

$\text{Bi}_{2+x}\text{Sr}_{2-x}\text{CuO}_y$ ($0.10 \leq x \leq 0.40$) polycrystalline samples have been studied by x-ray diffraction, resistivity and Hall-coefficient measurements, x-ray and ultraviolet photoemission spectroscopy, and inverse-photoemission spectroscopy (IPES). The lattice constant of the c axis decreases and that of the a (b) axis increases as a function of x . The results of Hall-coefficient measurements indicate that hole concentration is reduced as a function of x , which is consistent with the results of oxygen-concentration measurements. We find no energy shifts of the core levels, valence bands, and conduction bands for the samples, which is completely different from the results for the $\text{Bi}_2\text{Sr}_2\text{Ca}_{1-x}\text{Y}_x\text{Cu}_2\text{O}_y$ system. The results of IPES and resistivity measurements show that the metal-semiconductor transition occurs at about $x=0.35$. The states created by hole doping move to the Fermi level. The change in the electronic states is discussed.

INTRODUCTION

It is well known that high- T_c superconductivity is realized in the region of the insulator-metal transition by doping carriers into insulators, for example, by substitution of alkaline-earth metals for La in La_2CuO_4 (La-2:1:4) (Ref. 1) and by adding oxygen to $\text{YBa}_2\text{Cu}_3\text{O}_5$.² For bismuth cuprate high- T_c superconductors, holes are intrinsically doped by excess oxygen.³ However, the metal-insulator transition occurs with substitution of trivalent ions at Ca sites in $\text{Bi}_2\text{Sr}_2\text{CaCu}_2\text{O}_y$ (Bi-2:2:1:2).⁴

Changes in electronic structure caused by the metal-insulator transition have been studied using electron spectroscopy to understand the doping mechanism and electronic structures of strongly correlated compounds.⁵ It was found that most of the holes are doped into the O $2p_{x,y}$ orbital⁶ and the states at the Fermi level increase in intensity as a function of the holes doped.⁷ The chemical potential appears to be pinned for La cuprate.^{8,9} For the electron-doped cuprate $\text{Nd}_{2-x}\text{Ce}_x\text{CuO}_4$, no binding-energy shifts of core levels and valence bands were found as a function of Ce content.^{9,10} On the other hand, the binding energies of core levels and valence band were shifted to the high-binding-energy side as a function of Y content in $\text{Bi}_2\text{Sr}_2\text{Ca}_{1-x}\text{Y}_x\text{Cu}_2\text{O}_y$,^{11,12} leading to the model of a simple doped semiconductor.

$\text{Bi}_{2+x}\text{Sr}_{2-x}\text{CuO}_y$ (Bi-2:2:0:1) becomes a superconductor with $T_c = 10$ K at around $x = 0.1$,¹³ but the composition at which it becomes an insulator is not clear. The T_c

is increased to about 30 K by the substitution of rare-earth elements at Sr sites.¹⁴ This is a surprising increase compared with the Bi-2:2:1:2 system.¹⁵ The Bi-2:2:0:1 sample has the same CuO_2 structure as La-2:1:4 and it has the simplest structure in the $\text{Bi}_2\text{Sr}_2\text{Ca}_{n-1}\text{Cu}_n\text{O}_{6+2(n-1)}$ family. Therefore, we are interested in changes of the electronic states due to the substitution of trivalent Bi at divalent Sr sites.

In this paper, the results of systematic studies on the structure, resistivity, Hall coefficient, and oxygen concentration of Bi-2:2:0:1 samples is presented. The electronic states of the samples are also studied using x-ray (XPS), ultra-violet (UPS), and inverse-photoemission (IPES) spectroscopy.

EXPERIMENT

The $\text{Bi}_{2+x}\text{Sr}_{2-x}\text{CuO}_y$ polycrystalline samples ($0.10 \leq x \leq 0.40$) were synthesized by solid-state reaction of appropriate amounts of Bi_2O_3 , SrCO_3 , and CuO powder (99.9%). The mixed powder was pre-fired at 800°C for 12 h and at 820°C for 12 h in air. It was ground, pressed into pellets, and sintered at 850–870°C for 15 h in air.

The structure and homogeneity of the samples were examined by x-ray diffraction (XRD) and electron-probe microanalysis (EPMA), respectively. The precise lattice parameters were determined by using silicon single crystals as an internal standard. The resistivities and Hall

coefficients of the samples were measured by the standard methods between 15 and 300 K, and at 300 K, respectively. The oxygen concentration of some samples was determined by the iodine-titration method.

The samples were cleaned *in situ* by scraping in an ultrahigh-vacuum chamber (1×10^{-10} Torr) with a diamond field just before electron-spectroscopic measurements. XPS and UPS measurements were carried out using Al K_{α} (Perkin-Elmer, model 5100) and He I (VG Scientific) sources, respectively. Unoccupied electronic states were examined by detecting 9.6-eV photons using a home-made IPES apparatus.¹⁶ The Fermi energies for XPS and IPES were calibrated using Au $4f_{7/2} = 74.0$ eV and the Fermi edge of Pt, respectively.

RESULTS AND DISCUSSION

A. Characterization of the samples

All peaks in the XRD patterns of the $\text{Bi}_{2+x}\text{Sr}_{2-x}\text{CuO}_y$ samples ($x = 0.10$ and 0.40) were ascribed to the tetragonal structure. Changes of the lattice parameters along with the Hall coefficient are shown in Fig. 1(a) as a func-

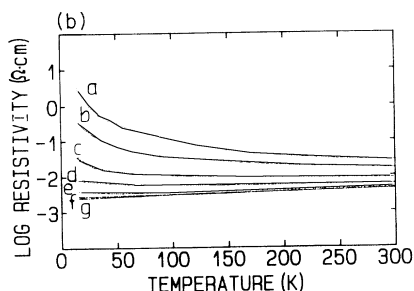
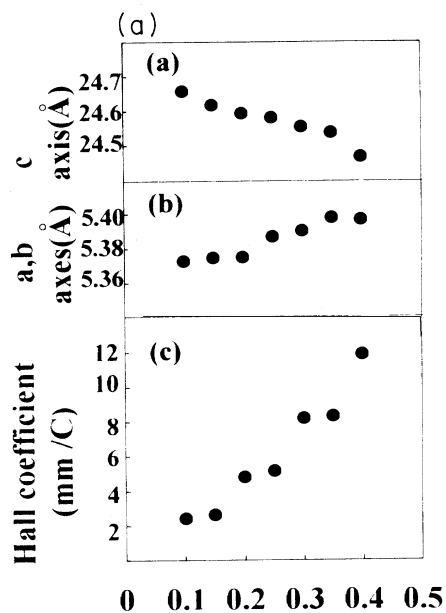


Fig. 1. (a) Changes in lattice parameters and Hall coefficients as a function of x in $\text{Bi}_{2+x}\text{Sr}_{2-x}\text{CuO}_y$. (b) Changes in resistivity (logarithm is base 10) as a function of temperature, where $x = 0.40$ (curve a), 0.35 (curve b), 0.30 (curve c), 0.25 (curve d), 0.20 (curve e), 0.15 (curve f), and 0.10 (curve g).

tion of x . The c and $a (=b)$ axes are systematically decreased and increased, respectively, as a function of x . The orthorhombic structure is not found, which is in agreement with previous results.¹³ The EPMA results (not shown here) indicated that the substitution of bismuth at strontium sites occurs homogeneously in each grain.

Changes in resistivity as a function of temperature are displayed in Fig. 1(b). The magnitude of T_c cannot be determined from the figure due to the limitation of the lowest temperature, but we can safely say that the samples with $x = 0.10$ and 0.15 behave as a metal. This is consistent with the result that the $\text{Bi}_{2.1}\text{Sr}_{1.9}\text{CuO}_y$ sample has $T_c = 10$ K.¹³ The resistivities at 300 K for $x = 0.10$ – 0.30 are not so much different, but those for $x = 0.35$ and 0.40 are one order of magnitude higher than the others, and these samples behave as a semiconductor at low temperature.

The Hall coefficients increase as a function of x , which implies that movable carriers are decreased by substitution. This is consistent with the changes of resistivity and reduction of hole concentration (discussed later) as a function of x .

B. Core-level electronic states

XPS spectra of Bi $4f$, Cu $2p_{3/2}$, and O $1s$ lines for $x = 0.15$ and 0.35 were measured. We found that the binding energies of Bi $4f_{7/2}$, Cu $2p_{3/2}$, and O $1s$ are 158.1 933.4, and 528.6 eV, respectively, which are in agreement with previous results.¹² They (including Sr $3d$) were not shifted by substitution. The full widths at half maximum (FWHM's) of the lines remained constant as x varied except for the O $1s$ line. The FWHM of the O $1s$ line for $x = 0.15$ was wider by 0.3 eV than that for $x = 0.35$.

It has been reported that the core-level binding energies of the constituent atoms in $\text{Bi}_2\text{Sr}_2\text{Ca}_{1-x}\text{Y}_x\text{Cu}_2\text{O}_y$ are shifted to the higher-binding-energy side with increasing x . This was discussed in terms of chemical-potential shifts,¹² which could be explained by a simple doping mechanism in semiconductors. On the other hand, the shifts were not observed for La-2:1:4 (Refs. 8 and 9) and Y-1:2:3 (Refs. 7 and 17) with increasing hole concentration, which cannot be explained by a simple band calculation.

A narrowing of the O $1s$ line was also observed for Bi-2:2:1:2 samples with substituted Y, and was attributed to the decrease in concentration of the oxygen orbital with holes.¹⁸ The FWHM of the O $1s$ line for the Bi-2:2:0:1 system also becomes narrower due to decrease of hole concentration with substitution. It should be emphasized here that the analysis of the O $1s$ line in the Bi-2:2:1:2 superconductors is also valid for the Bi-2:2:0:1 system.

C. Valence- and conduction-band electronic states

Many studies on the nature of the electronic states near the Fermi level (E_F) have been reported. It is well known¹⁹ that the valence-band spectra for Bi-2:2:1:2 and Bi-2:2:0:1 between E_F and about 7.5 eV measured by He I UPS ($h\nu = 21.2$ eV) mainly reflect the O $2p$ orbital be-

cause of the photoionization cross section at the photon energy. The experimental spectrum is in good agreement with the calculated spectrum.²⁰ Near the Fermi level in Bi-2:2:1:2 the spectrum was found²¹ by measuring the polarization-dependent energy-dispersion curve to have primarily O 2*p_x* and O 2*p_y* character; these orbitals are hybridized with the Cu 3*d* orbital. The states near *E_F* are reduced in intensity by increasing *x* in Bi₂Sr₂Ca_{1-x}Y_xCu₂O_y and a band gap opens.^{5,22} Our UPS and IPES results shown in Fig. 2 are in good agreement with those in Y-substituted Bi-2:2:1:2, although the sites occupied by the trivalent ions are different for the two samples. This implies that the electronic states are created by hole doping into the O 2*p* orbital. No band shifts for Bi-2:2:0:1 with substitution are observed in Fig. 2.

It has been reported that not only the core levels but also the valence band are shifted with the substitution of Y at Ca sites in Bi-2:2:1:2.^{11,12} These shifts were strongly dependent upon the hole concentration controlled by the Y content. The binding-energy shift in Bi-2:2:1:2 is compared with that in Bi-2:2:0:1 (this work) in Table I, as a function of hole concentration obtained by the iodine-titration method. The result indicates that the changes in hole concentration for both systems are similar but the binding-energy shift is completely different: about +0.2 eV shift for Bi-2:2:1:2 and no shift for Bi-2:2:0:1. This suggests that the Fermi level is pinned for variation of hole concentration, as in La_{2-x}Sr_xCuO₄ (Refs. 8 and 9) and YBa₂Cu₃O_{7-x},^{7,17} which implies that simple band theory cannot describe the electronic structures of this strongly correlated system. The disagreement of our result with that for Bi-2:2:1:2 might be due to difference in the sites substituted, the structure of the Cu-O planes, or the coupling between the CuO₂ and other layers.

IPES spectra are displayed as a function of *x* in Fig. 3. Peaks are found at about 0.5, 4, and 9 (not shown here) eV above the Fermi level, which is in close agreement with the O 1*s* spectrum obtained by x-ray-absorption spectroscopy for Bi-2:2:1:2,²³ and the IPES result for Bi-2:2:1:2.²⁴ The state near the Fermi level is generally recognized to be the O 2*p* state.²⁵ The bands at about

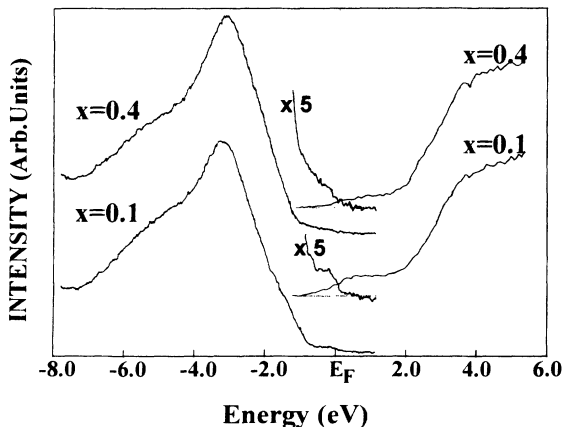


FIG. 2. HeI UPS ($h\nu=21.2$ eV) valence-band and IPES empty conduction-band spectra for $x=0.10$ and 0.40 .

TABLE I. Changes in excess oxygen (*d*), hole concentration, and Fermi-level shift as functions of *x* for Bi_{2+x}Sr_{2-x}CuO_{6+d} and Bi₂Sr₂Ca_{1-x}Y_xCu₂O_{8+d}.

<i>x</i>	<i>d</i>	Holes/CuO ₂	Fermi-level shift (eV)
Bi _{2+x} Sr _{2-x} CuO _{6+d}			
0.15	0.18	0.21	0
0.25	0.21	0.16	0
0.35	0.23	0.11	0
Bi ₂ Sr ₂ Ca _{1-x} Y _x Cu ₂ O _{8+d} ^a			
0.00	0.23	0.23	0
0.10	0.23	0.18	
0.30	0.30	0.15	0.18

^aReference 12.

3–4 eV were ascribed to Bi 6*p*,²⁴ and/or Cu 3*d* hybridized with the O 2*p* orbital.²³ The higher-energy band at about 8 eV would be due to Sr 4*d*-derived levels.²⁴

We find that the intensity at the Fermi level is significantly reduced at about $x=0.35$. This result, along with the resistivity data, suggests that the metal-semiconductor transition occurs at about $x=0.35$. The figures show that the peak at about 0.5 eV (indicated by arrows) is shifted to higher energy as *x* increases. On the other hand, the thresholds of the main band (indicated by the interpolation) are not shifted with *x*. This result suggests that the hole states are created at the top of the gap for light doping of holes, and the states extend to the Fermi level as hole concentration increases, leading to the result that the system becomes metallic.

A calculation has shown that the Fermi level is at the bottom or the top of the gap with *p*- or *n*-type doping, respectively,²⁵ which was also suggested by the electron energy loss spectroscopy (EELS).²⁶ However, this idea is

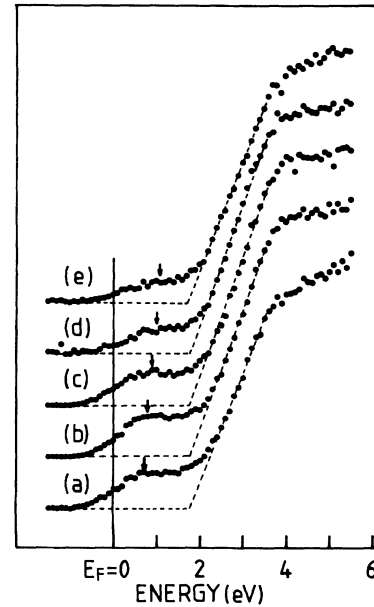


FIG. 3. IPES conduction-band spectra between $E_F=0$ and 6 eV, where $x=0.10$ (a), 0.15 (b), 0.30 (c), 0.35 (d), and 0.40 (e). The peaks near the Fermi level are indicated by the arrows and the main band edges are indicated by the interpolation.

not in agreement with the results of valence-band photoemission.⁹ The binding energy of $O\ 1s$ for $\text{Bi}_{2+x}\text{Sr}_{2-x}\text{CuO}_y$ (p type) is the same as that for $\text{Nd}_{2-x}\text{Ce}_x\text{CuO}_4$ (n type),¹⁰ which is not consistent with the above idea.

It was observed by measuring polarized $O\ 1s$ absorption spectra for single-crystal Bi-2:2:1:2 and for insulating Y -substituted samples (with Y concentration $x=0.6$) that a shoulder (upper Hubbard band) with in-plane symmetry occurs at 1 eV above the Fermi level for the insulator; this state is reduced by hole doping, and new states are created in the gap.²⁷ Our result does not indicate clear bands at 1 eV above the Fermi level for $x=0.40$, which is in agreement with the previous IPES results for a $\text{Bi}_2\text{Sr}_2\text{Ca}_{1-x}\text{Y}_x\text{Cu}_2\text{O}_y$ polycrystalline sample.²⁸ This would be due to the polycrystalline sample.

In summary, we have found that the c and a ($=b$) axes

decrease and increase continuously, respectively, as x increases in $\text{Bi}_{2+x}\text{Sr}_{2-x}\text{CuO}_y$, with a single phase of tetragonal structure. This result, along with the increase in Hall coefficient, indicates that substitution of trivalent Bi for divalent Sr occurs, which is consistent with the result that the resistivity changes from metallic to semiconducting with substitution. The binding energies of core levels are not shifted as a function of x , in contrast to those in $\text{Bi}_2\text{Sr}_2\text{Ca}_{1-x}\text{Y}_x\text{Cu}_2\text{O}_y$. The UPS spectra show that the Fermi edge is strongly reduced in intensity for $x=0.40$ and the valence band is not shifted with x . The absence of energy shifts of the core levels and valence bands suggests that the Fermi level of this system is pinned for variation in x . The empty states ($O\ 2p$ states) move to the Fermi level and the main band is not shifted as x varies, which suggests that the states are created at the top of the gap.

*Author to whom correspondence should be addressed.

¹For example, J. G. Bednorz and K. A. Müller, *Z. Phys. B* **64**, 189 (1986); S. Uchida, H. Takagi, H. Ishii, H. Eisaki, T. Yabe, S. Tajima, and S. Tanaka, *Jpn. J. Appl. Phys.* **26**, L440 (1987).

²For example, Z. Z. Wang, J. Clayhold, N. P. Ong, J. M. Tarascon, L. H. Greene, W. R. MaKinnon, and G. W. Hull, *Phys. Rev. B* **36**, 7222 (1987).

³For example, R. G. Buckley, J. L. Tallon, I. W. M. Brown, M. R. Presland, N. E. Flower, P. W. Glberd, M. Bowden, and N. B. Milestone, *Physica C* **156**, 629 (1988).

⁴T. Tamegai, A. Watanabe, K. Koga, I. Oguro, and Y. Iye, *Jpn. J. Appl. Phys.* **27**, L1074 (1988).

⁵For example, H. Matsuyama, T. Takahashi, H. K. Yoshida, T. Kashiwakura, Y. Okabe, S. Sato, N. Kosugi, A. Yagishita, K. Tanaka, H. Fujimoto, and H. Inokuchi, *Physica C* **160**, 567 (1989); Y. Fukuda, K. Terashima, Y. Nakanishi, T. Suzuki, M. Nagoshi, Y. Synono, and M. Tachiki, *ibid.* **162**, 1315 (1989).

⁶For example, F. J. Himpsel, G. W. Chandrashekar, A. B. McLean, and M. W. Shafer, *Phys. Rev. B* **38**, 11 946 (1988).

⁷For example, P. Kuiper, G. Knuizinga, J. Ghijsen, M. Grioni, P. J. W. Wejjs, F. M. F. de Groot, and G. A. Sawatzky, *Phys. Rev. B* **38**, 6483 (1988).

⁸Z. X. Shen, J. W. Allen, J. J. Yeh, J. S. Kang, W. Ellis, W. Spicer, I. Lindau, M. B. Maple, Y. D. Dalichaouch, M. S. Torikachivili, J. Z. Sun, and T. H. Geballe, *Phys. Rev. B* **36**, 8414 (1987).

⁹J. W. Allen, C. G. Olson, M. B. Maple, J. S. Kang, L. Z. Liu, J. H. Park, R. O. Anderson, W. P. Ellis, J. T. Markert, Y. Dalichaouch, and R. Liu, *Phys. Rev. Lett.* **64**, 595 (1990).

¹⁰Y. Fukuda, T. Suzuki, M. Nagoshi, Y. Synono, K. Oh-ishi, and M. Tachiki, *Solid State Commun.* **72**, 1183 (1989); T. Suzuki, M. Nagoshi, Y. Fukuda, K. Oh-ishi, Y. Synono, and M. Tachiki, *Phys. Rev. B* **42**, 4263 (1990).

¹¹R. Itti, F. Munakata, K. Ikeda, H. Yamauchi, N. Koshizuka, and S. Tanaka, *Phys. Rev. B* **43**, 6249 (1991).

¹²M. A. Van Veenendaal, R. Schlatmann, G. A. Sawatzky, and W. A. Groen, *Phys. Rev. B* **47**, 446 (1993).

¹³C. Michel, M. Hervieu, M. M. Borel, A. Grandin, F. Deslandes, J. Provost, and B. Raveau, *Z. Phys. B* **68**, 421 (1987); Y. Ikeda, H. Ito, S. Shimomura, Y. Oue, K. Inaba, Z.

Hiroi, and M. Takano, *Physica C* **159**, 93 (1989).

¹⁴For example, T. Kijima, J. Tanaka, and Y. Bando, *Jpn. J. Appl. Phys.* **27**, L1035 (1988); T. Den, A. Yamazaki, and J. Akimitsu, *ibid.* **27**, L1620 (1988).

¹⁵Y. Koike, Y. Yuwabuchi, S. Hosoya, N. Kobayashi, and T. Fukase, *Physica C* **159**, 105 (1989).

¹⁶N. Sanada, M. Shimomura, and Y. Fukuda, *Rev. Sci. Instrum.* **64**, 3480 (1993).

¹⁷H. Ihara, M. Jo, N. Terada, M. Hirabayashi, H. Oyanagi, K. Murata, Y. Kimura, R. Sugise, I. Hayashida, S. Ohashi, and M. Kimoto, *Physica C* **153-155**, 131 (1988).

¹⁸M. Nagoshi, Y. Fukuda, N. Sanada, Y. Synono, A. T. Yamamoto, and M. Tachiki, *J. Electron Spectrosc. Relat. Phenom.* **61**, 309 (1993).

¹⁹For example, T. Takahashi, H. Matsuyama, H. K-Yoshida, Y. Okabe, S. Hosoya, K. Seki, H. Fujimoto, M. Sato, and H. Inokuchi, *Nature* **334**, 69 (1988); M. Onellion, Ming Tang, Y. Chang, G. Margaritondo, J. M. Tarascon, P. A. Morris, W. A. Bonner, and N. G. Stoffel, *Phys. Rev. B* **38**, 881 (1988); Z. X. Shen, P. A. P. Lindberg, I. Lindau, W. E. Spicer, C. B. Eom, and T. H. Geballe, *ibid.* **38**, 7152 (1988).

²⁰P. Marksteiner, S. Massida, J. Yu, A. J. Freeman, and J. Redinger, *Phys. Rev. B* **38**, 5098 (1988).

²¹B. O. Wells, P. A. P. Lindberg, Z. X. Shen, D. S. Dessau, W. E. Spicer, and I. Lindau, *Phys. Rev. B* **40**, 5259 (1989).

²²T. Takahashi, H. Matsuyama, H. K. Yoshida, K. Seki, K. Kamiya, and H. Inokuchi, *Physica C* **170**, 416 (1990).

²³W. Drube, F. J. Himpsel, G. V. Chandrashekar, and M. W. Shafer, *Phys. Rev. B* **39**, 7328 (1989).

²⁴T. J. Wagener, Y. J. Hu, M. B. Jost, J. H. Weaver, Y. F. Yan, X. Chu, and Z. X. Zhao, *Phys. Rev. B* **42**, 6317 (1990).

²⁵P. Horsch, W. H. Stephan, K. V. Szczepanski, M. Ziegler, and W. Von der Linden, *Physica C* **162-164**, 783 (1989); P. C. Pattnaik and D. M. Newns, *Phys. Rev. B* **41**, 880 (1990); C. Melo and S. Doniach, *ibid.* **41**, 6633 (1990).

²⁶H. Romberg, M. Alexander, N. Nucker, P. Adelman, and J. Fink, *Phys. Rev. B* **42**, 8768 (1990).

²⁷T. Takahashi, S. Suzuki, T. Kusunoki, S. Sato, H. K. Yoshida, A. Yamanaka, F. Minami, and S. Takekawa, *Physica C* **185-189**, 1057 (1991).

²⁸T. Watanabe, T. Takahashi, S. Suzuki, S. Sato, and H. K. Yoshida, *Phys. Rev. B* **44**, 5316 (1991).